

## Magnetic moments in thin epitaxial Cr films on Fe(100)

P. Fuchs, V. N. Petrov,\* K. Totland, and M. Landolt

*Laboratorium für Festkörperphysik, Eidgenössische Technische Hochschule Zürich, CH-8093 Zürich, Switzerland*

(Received 26 February 1996)

The absolute magnetic moments of thin Cr overlayers on Fe(100) are directly determined by energy-resolved spin-polarized secondary-electron emission. Spin-dependent attenuation of low-energy secondary electrons is quantitatively treated, following a model by Siegmann, to extract magnetic depth profiles in the adlayer. The first monolayer of Cr couples antiferromagnetically to the Fe substrate and exhibits a maximum magnetic moment of  $1.8 \pm 0.2 \mu_B$  per atom for a submonolayer coverage. Subsequent Cr layers show a positive magnetization. [S0163-1829(96)06538-1]

The topic of induced magnetic moments in nonmagnetic adlayers at ferromagnetic surfaces combines state-of-the-art experimental thin film magnetometry with computational physics. Most important, however, is the quantitative experimental determination of the magnetic moments since the computers provide numerical values which are to be challenged. Stimulating indeed is the fact that on both sides even conceptual uncertainties persist and constant progress is made towards the understanding of the underlying physics.

In the present study we focus on Cr epitaxially grown on Fe(100) which is the best investigated system in its family. We utilize spin-polarized secondary-electron emission (SPSEE) as in a recent report on V/Fe(100).<sup>1</sup> The high surface sensitivity of SPSEE with a quantitative treatment of the spin dependence of the electron scattering enables us to extract quantitative magnetic moments of the adlayers. Substantial progress over the earlier study is made in that we utilize the energy dependence of the scattering and reach consistency as a stringent test. We find that at room temperature one monolayer (ML) of Cr on Fe aligns antiparallel to the Fe magnetization. It has a maximum magnetic moment of  $1.8 \pm 0.2 \mu_B$ /atom for a submonolayer coverage. Subsequent layers show a positive magnetization which decreases with increasing distance from the interface.

For a monolayer of Cr on Fe(100) an induced magnetization with very large magnetic moments ranging from 3.1 to  $3.9 \mu_B$ /atom (Refs. 2–4) has been predicted to align antiparallel to the magnetization of the Fe substrate accompanied by a slight reduction of the interfacial Fe moment. These early predictions so far could hardly be confirmed by experimental observations. For a submonolayer of Cr Idzerda *et al.* report  $0.6 \mu_B$ /atom from soft x-ray magnetic circular dichroism.<sup>5</sup> Hillebrecht *et al.*<sup>6</sup> have found from spin-polarized core-level photoemission a value of  $0.5$ – $1 \mu_B$ /atom. Hopster *et al.*<sup>7</sup> infer from an exchange splitting of 1.9 eV obtained by spin-polarized electron energy-loss spectroscopy a moment of roughly  $1.9 \mu_B$ /atom for 1 ML Cr on Fe. Later Turtur and Bayreuther have determined large magnetic moments of  $4 \mu_B$ /atom and a sizable depolarization of the Fe atoms at the interface by *in situ* alternating gradient magnetometry.<sup>8</sup> For Cr deposited on vicinal Fe surfaces the same group reports<sup>9</sup> strong deviations from the layered antiferromagnetic structure which are ascribed to particular surface morphologies. Recent tight-binding calculations claim<sup>10</sup> that the presence of

steps at the Cr-Fe interface leads to frustration and hence to multiple magnetic moment distributions with reduced average moments. This, however, contradicts first-principles band-structure calculations by Coehoorn<sup>11</sup> on Fe(100)/Cr superlattices with mixed monolayers at the interface where Fe and Cr moments show almost no dependence on the nearest-neighbor environment. A very recent study with spin-polarized core-level photoemission by Xu *et al.*<sup>12</sup> reports  $1.8 \mu_B$ /atom for a submonolayer coverage using the same polarization-to-moment conversion as in Ref. 6.

The SPSEE surface spectrometer<sup>13</sup> is straightforward. The sample, which is an Fe(100) single crystal with a Cr adlayer in the present case, is magnetized by a small horseshoe-shaped electromagnet along an easy direction. It exhibits full remanence at which all the measurements are performed. A secondary-electron cascade is excited near the surface by an unpolarized primary-electron beam of 2000 eV. The surface-normal emission of secondary electrons is resolved in energy in a cylindrical-mirror energy analyzer and subsequently submitted to spin-polarization analysis in a 100 keV Mott detector. The spin polarization is defined as  $P = (N\uparrow - N\downarrow) / (N\uparrow + N\downarrow)$ .  $N\uparrow(\downarrow)$  is the number of electrons with magnetic moment parallel (antiparallel) to the quantization axis of the detector which is chosen to lie parallel to the Fe magnetization direction. The Cr films are deposited on the well-prepared Fe(100) surface at room temperature by electron-beam evaporation. During evaporation the pressure is kept below  $10^{-9}$  Torr. The cleanliness of the substrate and of the adlayers is checked with Auger-electron analysis. The film thicknesses are determined by the relative changes of the Fe  $L_3M_{45}M_{45}$ , Fe  $M_{23}M_{45}M_{45}$ , and Cr  $L_3M_{23}M_{45}$  Auger-electron intensities upon evaporation. They exactly follow exponential attenuation laws as shown in Fig. 1, lower panel, with perfect consistency of the respective attenuation lengths<sup>14</sup> at the relevant energies. This gives evidence of a growth mode without island formation or interdiffusion. We do not expect, however, the growth to be strictly layer by layer. The absolute Cr thickness is based on published attenuation lengths.<sup>14</sup> The crystalline structure of the Cr layers is examined by low-energy electron-diffraction (LEED) analysis. We find that Cr on Fe(100) displays the same LEED pattern as clean Fe for all Cr thicknesses of the present study. The intensity maxima occur at the same electron energies as with Fe and no diffuse background is ob-

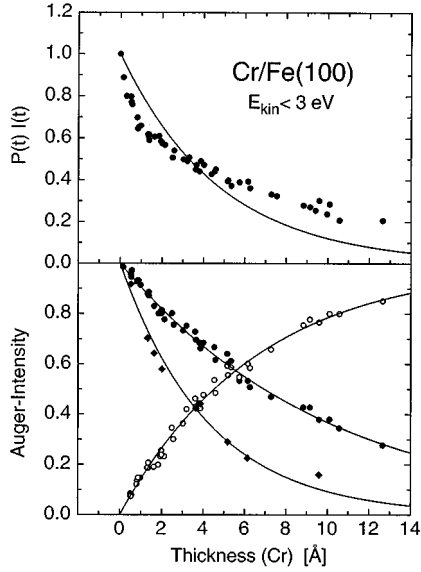


FIG. 1. Secondary-electron spin-polarization times intensity  $PI$  at  $E_{\text{kin}} < 3$  eV (upper panel) and Auger-electron intensities (lower panel) of Cr/Fe (100) versus Cr thickness. The solid lines represent exponentials with attenuation length  $\lambda = 4.7$  Å for  $PI$ , and 10 Å, 4.2 Å, and 6.5 Å for the Fe  $L_3M_{45}M_{45}$  (●), Fe  $M_{23}M_{45}M_{45}$  (◆), and Cr  $L_3M_{23}M_{45}$  (○) Auger lines, respectively.

served. Cr is adopting the structure of bcc-Fe. All measurements are performed at room temperature with a working pressure of  $(2-5) \times 10^{-10}$  Torr.

The measured secondary-electron spin-polarization  $P$  at low energies of a bulk sample is proportional to the sample magnetization in a surface region of about 4–5 Å (Ref. 15) thickness. The determination of the magnetic moment per atom  $\mu$  from  $P$  then requires quantitative knowledge of the production and emission rates of secondary electrons. For the production we can assume that all valence electrons are excited with equal probability  $i$ . This yields for each spin ( $\pm$  for up or down) a production rate of

$$i^{\pm} = i(n^{\pm} + n_{sp}/2), \quad (1)$$

where  $n^{\pm}$  and  $n_{sp}$  are the number of  $d$  and  $sp$  electrons, respectively, in the valence band. The emission from depth  $z$  then is governed by a spin-dependent inelastic scattering cross section  $\sigma^{\pm}$ . This gives rise to the secondary-electron current

$$dI^{\pm} = i^{\pm} \exp(-z\sigma^{\pm}) dz. \quad (2)$$

The key to the present magnetic moment determination lies in the quantitative treatment of  $\sigma^{\pm}$ . Following Siegmann and co-workers<sup>15</sup> the scattering cross section  $\sigma$  in transition metals can be described as being proportional to the number of  $d$  holes  $h = 2(5 - n)$  in the form

$$\sigma = \sigma_0 + \sigma_d(5 - n) \quad (3)$$

for sufficiently low kinetic energies of the electrons. The authors were able to determine the parameters  $\sigma_0$  and  $\sigma_d$  from a compilation of data of various transition metals. Straightforward application<sup>15</sup> of this concept to a ferromagnet then yields

$$\sigma^{\pm} = \sigma_0 \mp \sigma_d(n^+ - n^-)/2. \quad (4)$$

Using Eqs. (1)–(4) it is possible to express the observed spin polarization  $P$  in terms of  $n^{\pm}$ . This allows one to determine the magnetic moment which is given by  $\mu = (n^+ - n^-)\mu_B$  from  $P$  with only two adjustable parameters  $\sigma$  (or  $\sigma_0$ ) and  $\sigma_d$ .

Application of this scheme to a surface of a semi-infinite sample is not favorable since it assumes  $\mu$  to be constant for all depths  $z$  which usually is not the case. The power of the method, however, lies in the investigation of ultrathin adlayers in the submonolayer-to-monolayer range where the magnetization can be considered to be homogeneous over the adlayer thickness  $t$ . In the present study we use it to investigate Cr on Fe(100). In the case of an adlayer on a magnetic substrate the integration of Eq. (2) yields

$$I^{\pm}(t) = I_s^{\pm} \exp(-t\sigma^{\pm}) + i^{\pm} [1 - \exp(-t\sigma^{\pm})], \quad (5)$$

where  $I_s^{\pm}$  is the emission from the substrate. It appears to be practical to compute the quantity  $PI = I^+ - I^-$  in terms of the spin polarization of the valence electrons  $P_0 = (n^+ - n^-)/(n^+ + n^- + n_{sp})$  and compare it to the experimentally determined  $P(t)I(t)$ . The procedure has already been described in a recent study of V on Fe(100).<sup>1</sup> As a substantial progress, however, we here make use of the energy dependence of  $\sigma^{\pm}$ . At kinetic energies above 20 eV the spin dependence of the scattering cross section vanishes.<sup>16</sup> Thus we can compare data taken at below 3 eV and at 47 eV with the corresponding analyses using  $\sigma_d = 0.72$  nm<sup>-1</sup> (Ref. 15) and  $\sigma_d = 0$ , respectively. We indeed find a consistent picture which lends confidence to the validity of the scheme.

Using energy-resolved SPSEE we measure the spin polarization  $P$  and intensity  $I$  versus Cr thickness  $t$ . The observed thickness dependence of the product  $P(t)I(t)$  of secondary electrons with kinetic energies below 3 eV is presented in Fig. 1, upper panel. For a nonmagnetic overlayer it is expected to exhibit the exponential attenuation of the substrate emission by virtue of the overlayer. The signal strongly deviates however, from an exponential attenuation law with attenuation length  $\lambda = 4.7$  Å (Ref. 17) shown as a solid line in Fig. 1, upper panel. This is in pronounced contrast to the Auger intensities depicted in the lower panel of Fig. 1. The comparison with the Auger data demonstrates that the deviations of the  $PI$  signal from an exponential are of magnetic origin and do not relate to the growth properties of the adlayer. The difference between the  $PI$  data and the exponential background is shown in Fig. 2, upper panel. In principle it could arise from an induced magnetization in the Cr adlayer or from a considerable demagnetization of the substrate surface or a combination of the two. In the particular system Cr on Fe(100) only a weak depolarization of the interfacial Fe atoms compared to the bulk value is numerically predicted.<sup>2-4,12</sup> Moreover, element-specific measurements by core-hole photoemission of Cr on Fe(100) (Ref. 6) as well as of Fe on Cr(100) (Ref. 18) have shown that the Fe polarization and exchange splitting remain unchanged compared to pure Fe. Based on these observations we neglect a reduction of the magnetic moment of the Fe atoms at the interface. We note that with this assumption the present analysis yields an upper bound of the magnitude of the Cr moment. It further

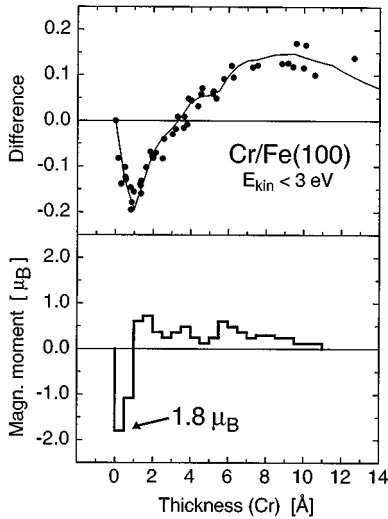


FIG. 2. (Upper panel) Secondary-electron spin-polarization times intensity  $PI$  at  $E_{\text{kin}} < 3$  eV of Cr/Fe (100) versus Cr thickness of Fig. 1 after subtraction of the exponential background. (Lower panel) Magnetization profile obtained from the data. The corresponding calculated  $PI$  (see text) is shown as a solid line in the upper panel.

turns out that consistency between the data of various electron energies only exists for zero reduction of the Fe interface moment.

Next we attempt to determine a magnetic depth profile from the  $PI$  data. As a first step starting from the bare substrate we calculate  $PI$  of a small Cr adlayer of thickness  $\delta$  within which we assume the moment to be constant. We use Eqs. (1)–(5) with the parameters  $\sigma = 1/\lambda$  and  $\sigma_d = 0.72 \text{ nm}^{-1}$  taken from Ref. 15 and obtain  $\mu$  of this Cr adlayer by best fit to the  $PI$  data. This step then is repeated for each additional fraction of adlayer of thickness  $\delta$  using the precedent layers of total thickness  $t$  as a new substrate. With this procedure we imply the rather strong assumption that the moment of a given layer does not change upon adsorption of further layers. The resulting magnetization profile  $\mu(t)$  is shown in Fig. 2, lower panel, together with the corresponding  $PI$  curve as a solid line in the upper panel.

In order to gain confidence in the quantitative treatment of the spin dependence of the inelastic scattering we have repeated the  $PI$  measurements at a different kinetic energy of the secondary electrons. Figure 3 shows  $PI$  at 47 eV kinetic energy as a function of the Cr thickness. This energy corresponds to the Fe  $M_{23}M_{45}M_{45}$  Auger line. It is particularly suited because the spin dependence of the scattering vanishes above 20 eV,<sup>16</sup> on one hand, and the attenuation length can directly be determined without further parameters from the decrease of the Auger intensity, on the other. The attenuation length turns out to be  $\lambda = 4.2 \text{ Å}$ . Deviations of  $PI$  from the corresponding attenuation law (solid line in Fig. 3, upper panel) again are significant; the difference is shown in the lower panel of Fig. 3. Using the same magnetic depth profile  $\mu(t)$  as in Fig. 2 obtained from low-electron-energy data we have calculated the thickness dependence of  $PI$  without any adjustable parameters taking  $\sigma = 1/\lambda$  and  $\sigma_d = 0$ . The result is shown as a solid line in the lower panel of Fig. 3. It exhibits good agreement with the experimental data. To illustrate the

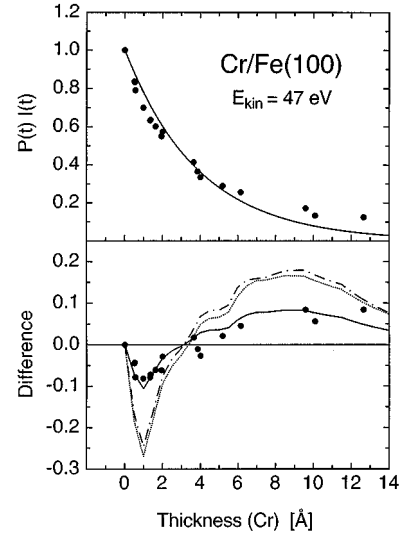


FIG. 3. Secondary-electron spin-polarization times intensity  $PI$  at  $E_{\text{kin}} = 47$  eV of Cr/Fe (100) versus Cr thickness. (Upper panel) raw data (dots) and exponential background with attenuation length  $\lambda = 4.2 \text{ Å}$  (solid line). (Lower panel) Same data after subtraction of the exponential background. The solid and broken lines represent  $PI$  calculations with different parameters of the model (see text).

sensitivity of  $PI$  to spin-dependent scattering we, for comparison, also have calculated  $PI$  with  $\sigma_d = 0.72 \text{ nm}^{-1}$  as in the low-energy case. The result (dotted line in Fig. 3) strongly deviates from the experimental data. Likewise as a test we have computed a profile  $\mu^*(t)$  from the low-energy  $PI$  data setting  $\sigma_d = 0$ , i.e., neglected spin-dependent scattering altogether.  $\mu^*$ , which is not shown here, exhibits qualitatively the same shape as  $\mu(t)$  but the absolute values are more than twice as large [ $-4.2 \mu_B$  for 0.3 ML Cr on Fe(100)]. The corresponding  $PI$  curve at 47 eV, however, does not fit the experimental data at all (dash-dotted line in Fig. 3). This indicates that spin-dependent scattering at low energies is important, indeed. The consistency of  $\mu(t)$  of Fig. 2 for both energies with and without scattering, respectively, demonstrates that the present treatment of spin-dependent attenuation is meaningful.

We have shown that the presence of the Fe interface induces a large spin polarization in thin Cr adlayers. For the particular structure of epitaxially grown Cr on Fe (100) at room temperature we find that a Cr adlayer of a submonolayer coverage has an induced magnetization of  $1.8 \pm 0.2 \mu_B$  per atom and is magnetically oriented antiparallel to the Fe surface magnetization. The entire  $\mu(t)$  in Fig. 2 can be regarded as a magnetic depth profile of Cr on Fe (100), but only with some reservation. We note that a reasonable fit to the data within the first monolayer only is obtained when using fractional monolayers. This reflects the fact that the growth at room temperature is not strictly layer by layer, as has been shown with tunnel microscopy.<sup>19</sup> The analysis furthermore implies the rather strong assumption that the magnetic moment in a given fraction of the Cr layer does not change upon adsorption of further layers. This assumption is correct for the first monolayer but, however, might be wrong for the next few layers near the Fe interface. We emphasize, however, that in the range of submonolayer coverage the determination of the magnetic moment for thin Cr films on

Fe (100) is a firm result. When going to thicker Cr adlayers we observe the sign of the induced magnetization to change in the first layer and the magnetization to remain positive for thicker Cr films.

It is a pleasure to thank H. C. Siegmann for many fruitful conversations and continuous support and to K. Brunner for expert technical assistance. Financial support by the Schweizerischer Nationalfonds is gratefully acknowledged.

\*Permanent address: Division of Experimental Physics, Technical University St. Petersburg, 195251 St. Petersburg, Russia.

<sup>1</sup>P. Fuchs, K. Totland, and M. Landolt, *Phys. Rev. B* **53**, 9123 (1996).

<sup>2</sup>C. L. Fu, A. J. Freeman, and T. Oguchi, *Phys. Rev. Lett.* **54**, 2700 (1985).

<sup>3</sup>R. H. Victora and L. M. Falicov, *Phys. Rev. B* **31**, 7335 (1985).

<sup>4</sup>J. Dorantes-Dávila *et al.*, *Surf. Sci.* **251/252**, 51 (1991).

<sup>5</sup>Y. U. Idzerda *et al.*, *J. Appl. Phys.* **73**, 6204 (1993).

<sup>6</sup>F. U. Hillebrecht, Ch. Roth, R. Jungblut, E. Kisker, and A. Bringer, *Europhys. Lett.* **19**, 711 (1992); R. Jungblut, Ch. Roth, F. U. Hillebrecht, and E. Kisker, *J. Appl. Phys.* **70**, 5923 (1991).

<sup>7</sup>T. G. Walker, A. W. Pang, H. Hopster, and S. F. Alvarado, *Phys. Rev. Lett.* **69**, 1121 (1992); H. Hopster (private communication).

<sup>8</sup>C. Turtur and G. Bayreuther, *Phys. Rev. Lett.* **72**, 1557 (1994).

<sup>9</sup>S. Miethaner and G. Bayreuther, *J. Magn. Magn. Mater.* **148**, 42 (1995).

<sup>10</sup>P. Martin, A. Vega, C. Demangeat, and H. Dreyssé, *J. Magn. Magn. Mater.* **148**, 177 (1995).

<sup>11</sup>R. Coehoorn, *J. Magn. Magn. Mater.* **151**, 341 (1995).

<sup>12</sup>Zhongde Xu, Y. Liu, P. D. Johnson, and B. S. Itchkawitz, *Phys. Rev. B* **52**, 15 393 (1995).

<sup>13</sup>M. Landolt, R. Allenspach, and D. Mauri, *J. Appl. Phys.* **57**, 3626 (1985).

<sup>14</sup>M. D. Seah and W. A. Dench, *Surf. Interface Anal.* **1**, 1 (1979).

<sup>15</sup>H. C. Siegmann, *J. Phys. Condens. Matter* **4**, 8395 (1992); G. Schönhense and H. C. Siegmann, *Ann. Phys.* **2**, 465 (1993).

<sup>16</sup>H. Hopster, R. Raue, E. Kisker, G. Güntherodt, and M. Campagna, *Phys. Rev. Lett.* **50**, 70 (1983); D. Mauri, R. Allenspach, and M. Landolt, *J. Appl. Phys.* **58**, 906 (1985).

<sup>17</sup> $\lambda=4.7 \text{ \AA}$  is obtained from intensity data of the present study. It compares well with  $\lambda=4.4 \text{ \AA}$  from Ref. 15.

<sup>18</sup>E. Beaurepaire *et al.*, *Surf. Sci.* **251/252**, 36 (1991).

<sup>19</sup>D. T. Pierce, J. A. Stroschio, J. Unguris, and R. J. Celotta, *Phys. Rev. B* **49**, 14 564 (1994).